Mesozoic 002 (1): 060–069
https://www.mapress.com/mz/

Article

ISSN 3021-1859 (print edition)
MESOZOIC
ISSN 3021-1867 (online edition)

https://doi.org/10.11646/mesozoic.2.1.8
http://zoobank.org/urn:lsid:zoobank.org:pub:F48952BF-2E4D-470A-BDF2-2893A1104E23

Distribution and mineralogical characteristics of amber in the Upper Cretaceous Gaogou Formation in Xixia, Henan Province, China

GAO-ZHE JI[1,2], CHEN-YANG CAI[1], XUE-FEI YU[3], DANY AZAR[1,4], CHONG DONG[1], XIANG-BO SONG[1], YE-HAO WANG[1], MIN-MIN XU[1] & DI-YING HUANG[1,*]

[1]*State Key Laboratory of Palaeobiology and Stratigraphy, Nanjing Institute of Geology and Palaeontology, Chinese Academy of Sciences, Nanjing 210008, China*
[2]*University of Chinese Academy of Sciences, Beijing 100049, China*
[3]*Liangyungang Comprehensive Inspection Testing Center of Quality Technology, Lianyungang 222000, China*
[4]*Faculty of Sciences II, Natural Sciences Department, Lebanese University, Fanar-El-Matn, PO Box 90656 Jdeideh, Lebanon*
gzji@nigpas.ac.cn; https://orcid.org/0000-0003-4496-9529
cycai@nigpas.ac.cn; https://orcid.org/0000-0002-9283-8323
168367409@qq.com; https://orcid.org/0009-0000-6235-5147
danyazar@ul.edu.lb; https://orcid.org/0000-0002-4485-197X
cdong@nigpas.ac.cn; https://orcid.org/0000-0001-9983-4352
xbsong@nigpas.ac.cn; https://orcid.org/0009-0009-7153-1005
yhwang@nigpas.ac.cn; https://orcid.org/0000-0002-4638-974X
mmxu@nigpas.ac.cn; https://orcid.org/0009-0002-6986-2883
dyhuang@nigpas.ac.cn; https://orcid.org/0000-0002-5637-4867
**Corresponding author*

Abstract

The Xixia amber is the largest known Mesozoic amber deposit in China to date. Here we analyse amber collected over the years from 12 localities in the Upper Cretaceous Gaogou Formation in Xixia, Henan, including physical property tests and Fourier transform infrared spectroscopy (FT-IR) analysis. The main preservation forms of the Xixia amber include nest-like, vein-like, and layered irregular shapes, as well as gravel-like forms resulting from secondary transportation. Recent discoveries include numerous small-grained amber specimens preserved in grey-black silty shale rich in plant debris, suggesting a near-in-situ depositional environment. The Xixia Basin's Late Cretaceous strata are renowned for their abundance in dinosaur eggs. In-depth research on the Xixia amber will help to understand the geological history and ecosystem evolution of the Xixia Basin during the Late Cretaceous, as well as the global distribution characteristics of Cretaceous amber.

Key words: Xixia amber, Xixia Basin, Late Cretaceous, FT-IR analysis

Introduction

Cretaceous amber is relatively scarce compared to Cenozoic amber, primarily distributed over a span of 54 million years from the Barremian to the Campanian. This period is now regarded as the Cretaceous Resinous Interval, as its biological inclusions play a crucial role in understanding the Cretaceous Terrestrial Revolution, as well as the palaeoclimate, palaeoenvironment, and palaeoecology of the late Mesozoic (Delclòs *et al*., 2023).

Recent years have seen significant progress in amber research in China, such as studies on bioinclusions in Eocene Fushun amber and Miocene Zhangpu amber (Wang *et al*., 2014; Wang *et al*., 2021). Previously, Cretaceous amber in China was rarely found outside of the Xixia amber, but a series of new discoveries have been made in recent years, including ambers from the late Aptian to early Albian in the Hulunbuir region of Inner Mongolia, encompassing Manzhouli and Hailar (Azar *et al*., 2019; Li *et al*., 2023; Gao *et al*., 2024). Late Cretaceous amber has also been discovered in the Upper Cretaceous Dalangshan Formation of Guangzhou City and the Yetang Formation of Xingning County in eastern Guangdong (Ni *et al*., 2023; Song *et al*., 2024).

Xixia County is located in central China, in the south-western part of Henan Province. The Late Cretaceous amber found here represents the largest Mesozoic amber deposit in China. Although the Xixia amber has been discovered in significant quantities, research on it remains limited (Wang, 1989; Zhong, 2003; Zhou & Zhao, 2005;

 Submitted: 16 Mar. 2025; accepted by Z. Feng: 22 Mar. 2025; published: 28 Mar. 2025

Chai & Huang, 2011; Shi *et al*., 2014; Li *et al*., 2024). The discovery and use of the Xixia amber date back over a thousand years, with large-scale collection occurring in the last century, primarily for use in traditional Chinese medicine. The Xixia amber boasts substantial production, with amber deposits varying in size and often consisting of a mixture of sediment and amber. The deposits are primarily small pockets, ranging from a few kilograms to between 10 and 150 kg. Larger single pockets typically weigh between 1300 and 3000 kg. Wuliqiao Town once yielded a pocket weighing 3374 kg, with the largest single piece weighing 100 kg, reportedly preserved in the Shanghai Museum (Zhou & Zhao, 2005; the authors were unable to locate this amber during visits to the Shanghai Museum and Shanghai Natural History Museum). By 2003, the total weight of amber mined from Xixia exceeded 5000 kg (Zhong, 2003). Due to its preservation in relatively hard sandstone, explosives were required for extraction. However, strict controls on explosives in the 21st century, coupled with the declining medicinal value of amber (locally used for haemostasis), have led to a significant reduction in amber mining in the Xixia region. Additionally, the Xixia amber is brittle and difficult to craft into artifacts, and no definitive biological inclusions have been reported, resulting in limited attention to this resource.

Wang (1989) tested on the physical properties, chemical properties, infrared and ultraviolet spectra, and XRD patterns of the Xixia amber, and briefly discussed its geological genesis. Zhou & Zhao (2005) provided a concise description of the characteristics of the Xixia amber deposit, including its mining and occurrence, and proposed that the amber originated from Late Triassic strata to the northwest and north of the basin, having undergone long-distance transport. Chai & Huang (2011) investigated the thermal behaviour of the amber, observing that the characteristic peaks generated by the stretching and bending vibrations of saturated hydrocarbon bonds changed with increasing temperature. Shi *et al*. (2014) identified terpenoid compounds in the Xixia amber and, based on biomarkers, inferred its botanical origin to be Araucariaceae gymnosperms. Li *et al*. (2024) carried out a comprehensive examination on Xixia amber, including microscopic observation, infrared spectroscopy, three-dimensional (3D) fluorescence spectroscopy, and pyrolysis gas chromatography-mass spectrometry (Py-GC-MS), and made a comparison of the yellow samples with yellow ones from Burmese, Fushun, and Baltic. The results revealed that the gemological traits of Xixia amber are similar to the ambers with the same colour from other origins, but it shows significant differences in infrared spectral characteristics from amber of other origins. Furthermore, the fluorescence behavior of Xixia amber is closer to that of Burmese and Fushun amber rather than Baltic amber. The py-GC-MS results account for this similarity, indicating that all three are characterized by a regular configuration and the absence of succinic acid.

Through years of field surveys in the amber-producing areas of Xixia, this paper reports on 12 amber localities within the Xixia Basin and presents tests and analyses conducted on these amber samples, laying the groundwork for further in-depth studies.

Geological setting

The Xixia Basin is primarily located in Xixia County, Henan Province, extending westward into Neixiang County. It is orientated NW-SE, with a trend of NW 295°, spanning approximately 100 km from east to west and 5–13 km in width from north to south. The basin is narrower in the west and wider in the east, covering an area of about 1000 km². It is a fault-controlled, half-graben-style basin (Li *et al*., 2006; Wang *et al*., 2008). The sedimentary strata consist exclusively of Late Cretaceous continental red beds, which generally overlie the Devonian Nanwan Formation. The periphery of the basin is characterized by metamorphic and magmatic rocks from the Qinling orogenic belt (Zhou *et al*., 2001) (Fig. 1B).

The Late Cretaceous continental red beds of the Xixia Basin formed under relatively arid climatic conditions (Zhang & Pei, 2004; Wang *et al*., 2015; He *et al*., 2020). From bottom to top, the strata are divided into the Gaogou Formation, Majiacun Formation, and Sigou Formation. These formations share similar lithologies and are conformably deposited, primarily composed of alluvial fan-fluvial facies conglomerate sandstones and siltstones (Henan Provincial Bureau of Geology and Mineral Resources, 1997; Zhu, 1997). The Gaogou Formation consists of conglomerates, medium- to coarse-grained sandstones interbedded with conglomerates, fine- to coarse-grained sandstones, and alternating purplish-red silty mudstones and siltstones. It is renowned for its abundant and well-preserved dinosaur egg fossils, as well as dinosaur bones and track fossils (Zhu, 1997; Wang *et al*., 2012). Dinosaur egg fossils in the Gaogou Formation are found at the bottom, middle, and top of the formation, while amber is typically produced in the sandstones above the middle dinosaur egg layer (Zhu, 1997; Zhou & Zhao, 2005). The Majiacun Formation is mainly composed of conglomerate sandstones, sandstones, and mudstones, with its middle section also containing numerous dinosaur egg fossils. Amber is also found in the fine sandstones of its lower section. The Sigou Formation consists of sandy conglomerates, fine sandstones, and silty mudstones, which also yield dinosaur eggs and amber (Zhu, 1997).

These red beds are all conformably deposited, making it difficult to determine specific stratigraphic affiliations based solely on lithology in the field. By projecting the locations of amber sites onto a geological map, we found that all the amber is produced in the Upper Cretaceous Gaogou Formation of the Xixia Basin, consistent with the formation's trend and distributed in a NWW direction (Fig. 1B). Amber has also been recorded in Neixiang County (Zhou & Zhao, 2005), but no further studies have been conducted.

Volcanic activity in the Xixia Basin during the Late Cretaceous appears to have been limited. Data indicate that the Gaogou Formation and Majiacun Formation in the Xixia Basin contain more than 20 layers of volcanic tuff (Zhou *et al*., 2002), but no precise dating has been published. In the Wulichuan Basin to the north-west of the Xixia Basin, the Upper Cretaceous Zhuyangguan Formation is developed, with a granite vein intruding its middle section. A K-Ar dating of muscovite yielded an age of ~70 Ma (Yang, 1987), indicating that the Zhuyangguan Formation red beds are no younger than the middle Maastrichtian. However, this data provides limited constraints on the age of the amber-bearing layers.

The dinosaur egg fossils, sporopollen, and charophyte fossils discovered in the Upper Cretaceous of the Xixia Basin exhibit assemblage characteristics similar to those of the Nanxiong Formation in Guangdong, the Wangshi Formation in Shandong, the Mingshui Formation in the Songliao Basin, and the Subashi Formation in Xinjiang, representing biological assemblages from the Late Cretaceous. Based on stratigraphic relationships, the Gaogou Formation is assigned to the early Late Cretaceous (Cenomanian to Turonian), the Majiacun Formation to the middle Late Cretaceous (Coniacian to Santonian),

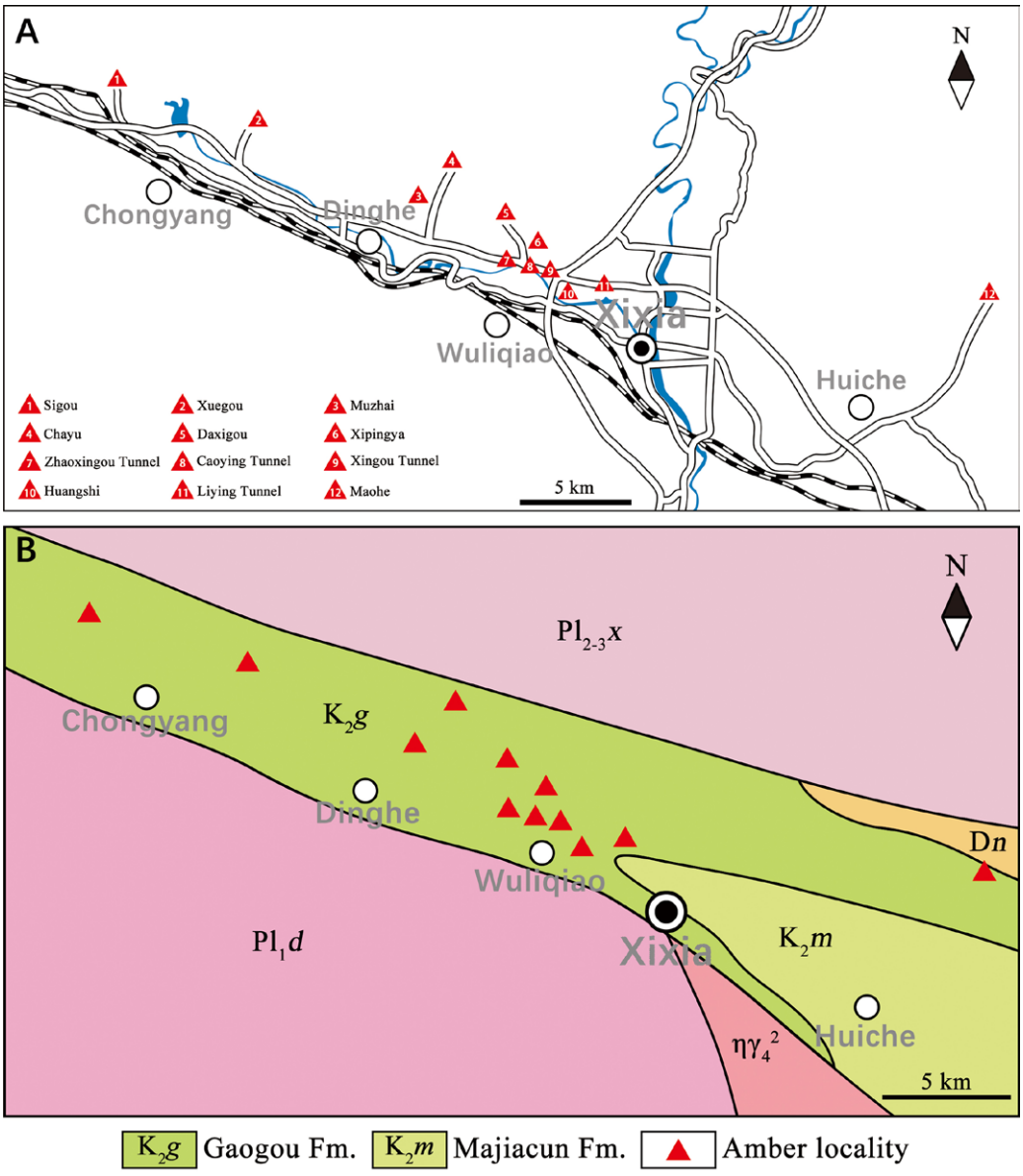

FIGURE 1. Amber localities. **A**, Locality map (red triangles indicating amber outcrops). **B**, Geological map.

and the Sigou Formation to the late Late Cretaceous (Campanian to Maastrichtian) (Zhou *et al*., 1983; Zhu, 1997). According to the bivalves and ostracods from these three formations, this set of red beds can be classified as belonging to the Coniacian to Campanian interval (Chen *et al*., 2007; Cao & Wang, 2011).

Material and methods

In this study, 12 amber-producing localities in the Xixia Basin were identified, including Sigou and Xuegou in Chongyang Township, Muzhai and Chayu in Dinghe Township, Daxigou, Xipingya, Zhaoxingou Tunnel, Caoying Tunnel, Xingou Tunnel, Liying Tunnel, and Huangshi in Wuliqiao Township, and Maohe in Huiche Township (Fig. 1A). We analysed amber samples collected from nine of these localities—Sigou, Muzhai, Xipingya, Daxigou, Zhaoxingou Tunnel, Caoying Tunnel, Xingou Tunnel, Liying Tunnel, and Huangshi (Fig. 2)—using Fourier transform infrared spectroscopy (FT-IR analysis), refractive index, hardness, density, and fluorescence response measurements.

Preservation

Xixia amber is primarily preserved in three forms: 1) Irregular preservation: the amber often appears in irregular shapes such as bands, veins, and lenses. This type of amber is typically mixed with sediments like sand and mud, forming larger amber-sediment mixtures, which are the most common form of amber production in Xixia. Locally, these are referred to as "amber nests" (Fig. 4); 2) gravel-like preservation (Fig. 2D): This form represents secondary transport and deposition, where the amber is preserved as well-rounded gravel within sandstone. The grain size is usually around 1 cm, with good sorting; and 3) near-in-situ preservation (Fig. 5): This type of amber was discovered at the Xipingya locality, where it is preserved in grey-black silty shale rich in plant debris, appearing as granular particles of varying sizes. This likely indicates that the amber underwent limited transport and experienced proximal deposition, consistent with preservation near its source environment.

Mineralogical Analysis

The density of the amber samples was measured using the hydrostatic method with an AL104 electronic balance. The refractive index was determined using refractive oil

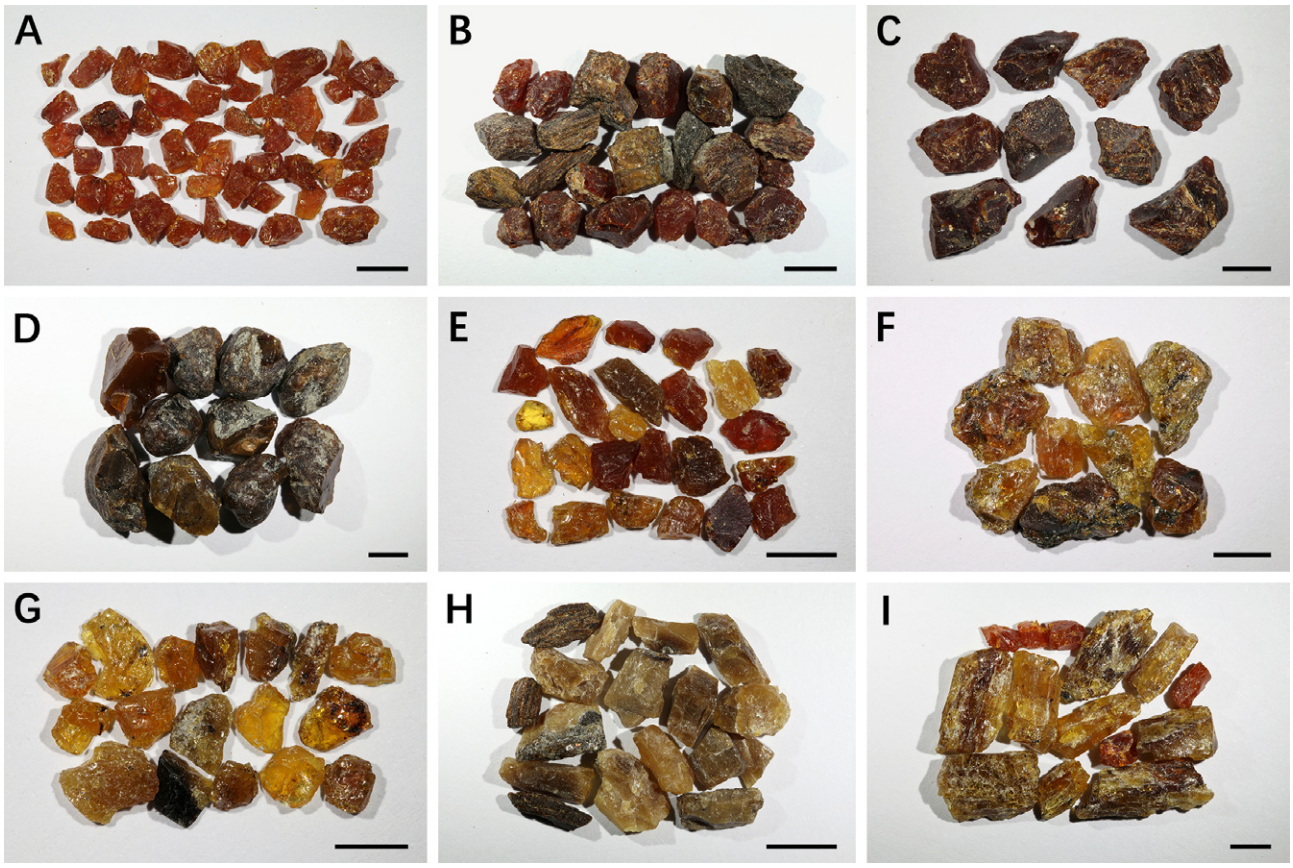

FIGURE 2. Amber samples from the Gaogou Formation. **A**, Amber from Xipingya. **B**, Amber from Daxigou. **C**, Amber from Sigou. **D**, Amber from Zhaoxingou Tunnel. **E**, Amber from Muzhai. **F**, Amber from Huangshi. **G**, Amber from Liying Tunnel. **H**, Amber from Caoying Tunnel. **I**, Amber from Xingou Tunnel. Scale bars = 0.5 cm.

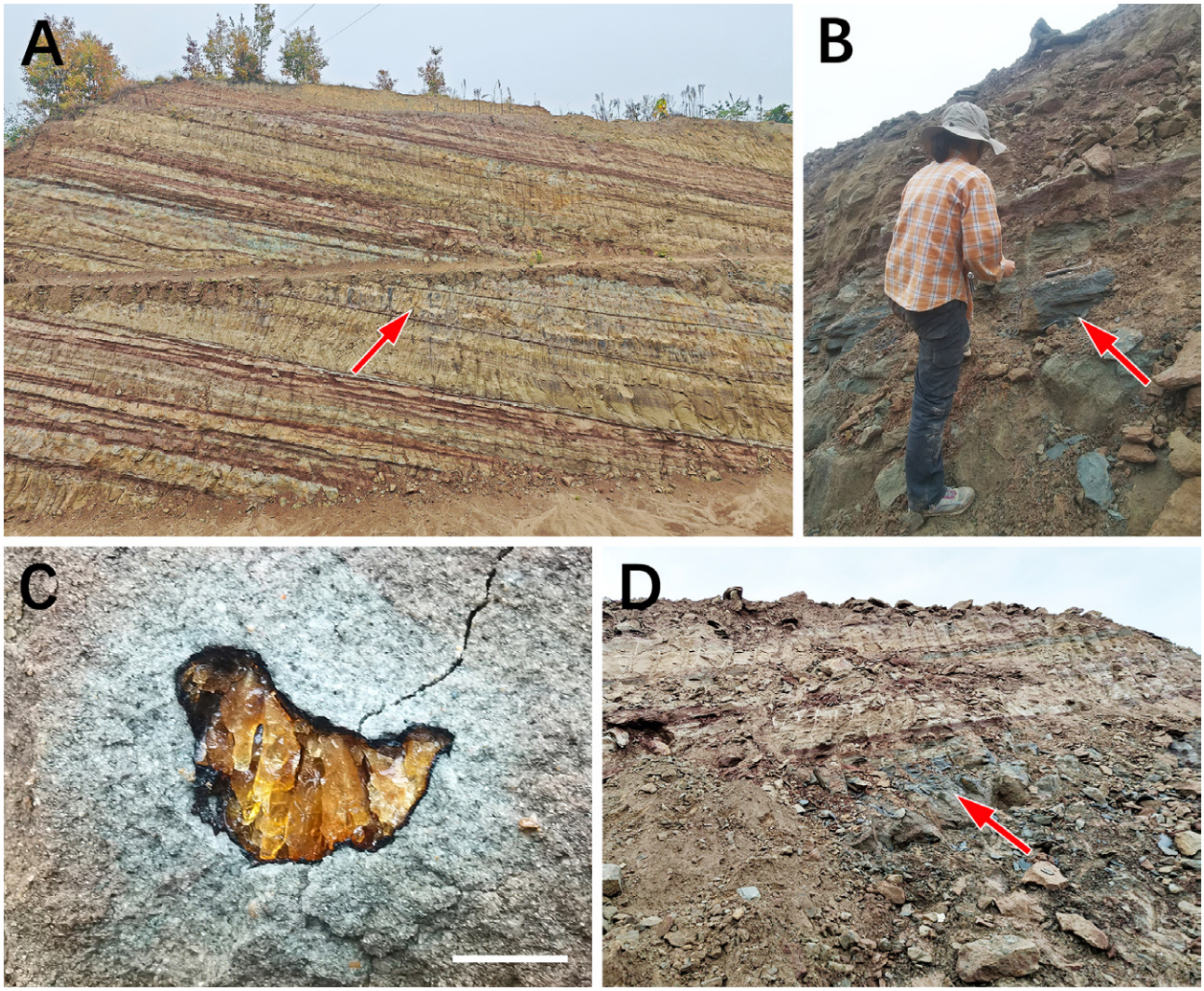

FIGURE 3. Xipingya outcrop. **A**, Xipingya section. **B**, Amber collecting. **C**, Amber from Xipingya. Scale bar = 1 cm. **D**, Amber layer.

in an Abbe-type gem refractometer. Mohs hardness was measured by scratching the samples with a hardness tester. Fluorescence effects were recorded under UV light using a UV fluorescence instrument.

FT-IR Analysis

For the infrared analysis, amber from each site was crushed and mixed with potassium bromide (KBr). Pellets were prepared using a hydraulic manual press. Spectra were acquired between 4000 and 400 cm^{-1}, with 40 scans collected at a resolution of 4 cm^{-1}. Transmission FT-IR spectroscopy was performed using a Bruker VERTEX spectrophotometer.

Photography

The photographs used for illustration were taken with a digital camera attached to a Zeiss Discovery V20 microscope and a Canon 5D Mark II camera equipped with a 100 mm macro lens. Fluorescence photographs were taken using the Canon camera under UV light. Maps were created using CorelDraw 2021 software. FT-IR spectra were generated using Origin 2024 software.

Results

Mineralogical characteristics

The Xixia amber exhibits variable transparency, ranging from golden-transparent to black, with colors including golden yellow, brownish yellow, orange-red, brownish red, dark red, brown, and black (Fig. 2). Four selected samples from three localities were labelled as XPY-01, SG-01, SG-02, and ZXG-01. After testing, their mineralogical properties were obtained (Table 1).

TABLE 1. Mineralogical characteristics of Xixia ambers.

Sample	Locaity	Refractive	Density	Hardness	Fluorescence	
					LW	SW
XPY-01	Huangshi	1.542	1.06	2.2	Strong	Weak
SG-01	Sigou	-	1.10	2.2	Weak	No
SG-02	Sigou	-	1.10	2.2	Middle	No
ZXG-04	Zhaoxingou Tunnel	-	1.02	2.5	Strong	Middle

*Hardness refers to Mohs hardness. LW refers to long-wave (365 nm). SW refers to short-wave (253.7 nm).

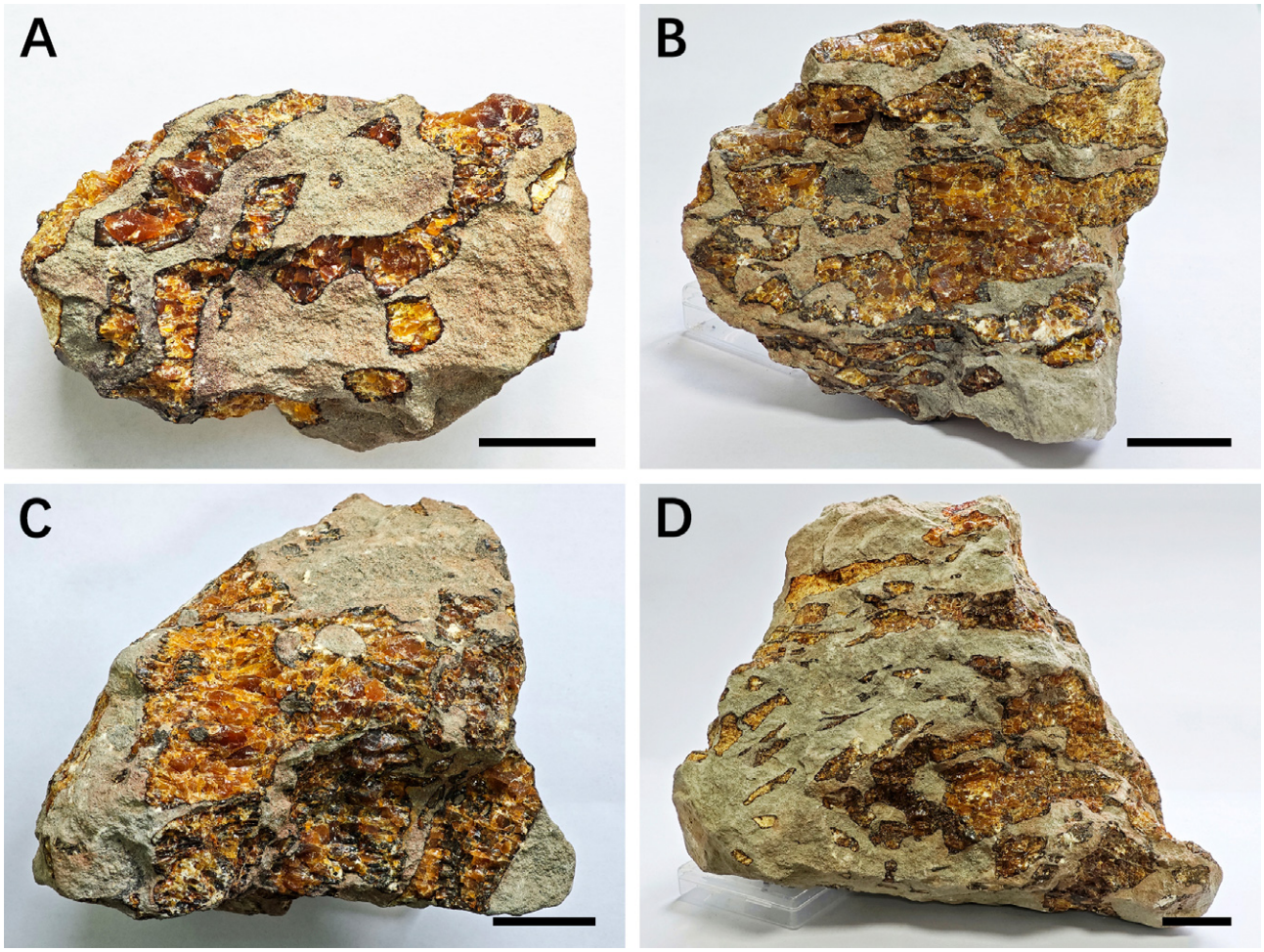

FIGURE 4. Photographs of amber pockets (part). Scale bars = 2 cm in **A**, 3 cm in **B**, **C**, **D**.

The tested samples have densities ranging from 1.02 to 1.10, with variations likely due to impurities and tiny bubbles within the amber. The Mohs hardness is generally 2.2, and the refractive index is approximately 1.542. Under long-wave ultraviolet fluorescence (365 nm), Xixia amber exhibits medium to strong fluorescence, appearing light blue, while weathered amber surfaces display a bluish-green fluorescence (Fig. 6). The reaction under short-wave ultraviolet fluorescence (253.7 nm) is relatively weak.

FT-IR Analysis

Fourier Transform Infrared (FT-IR) spectroscopy spectra were obtained from different amber materials to retain their chemical signatures and compare their chemical structure profiles. We chose to undertake such analyses despite the fact that they are of limited importance today, as most amber FT-IR spectra are more or less similar and do not provide precise data for resolving the botanical origin of the fossil resin (Azar *et al*., 2010). The spectra were acquired between 4000 and 400 cm^{-1}, with 40 scans collected at a resolution of 4 cm^{-1}. The spectra, ranging from 4000 to 400 cm^{-1}, can be divided into two regions: transmittance bands between 3700–1350 cm^{-1}, which are shared by almost all types of amber; and transmittance bands between 1350 and 400 cm^{-1}, generally considered the fingerprint region.

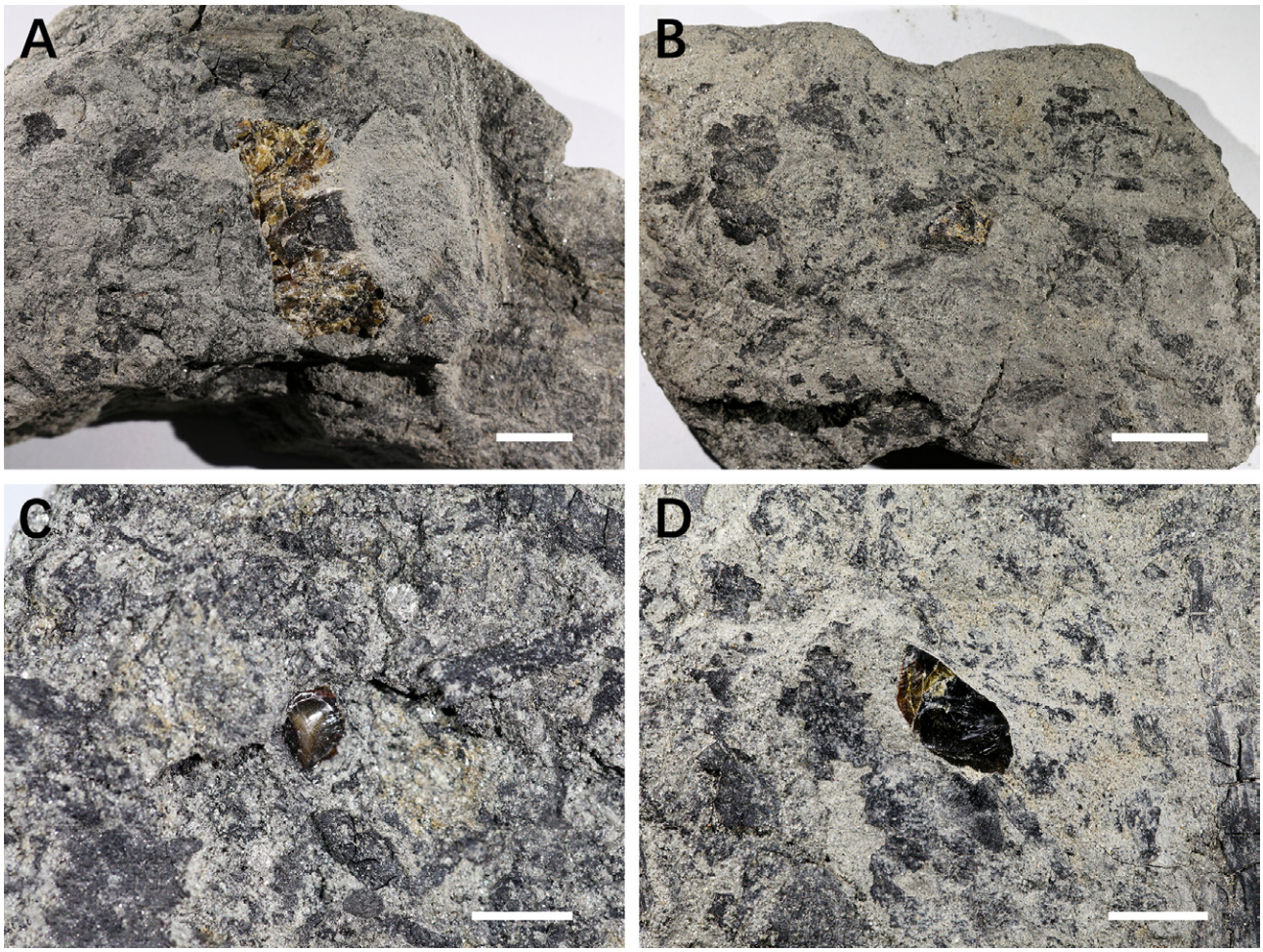

FIGFURE 5. Photographs of ambers with grey-black silty shale. Scale bars = 1 cm in **A**, **B**, 0.5 cm in **C**, **D**.

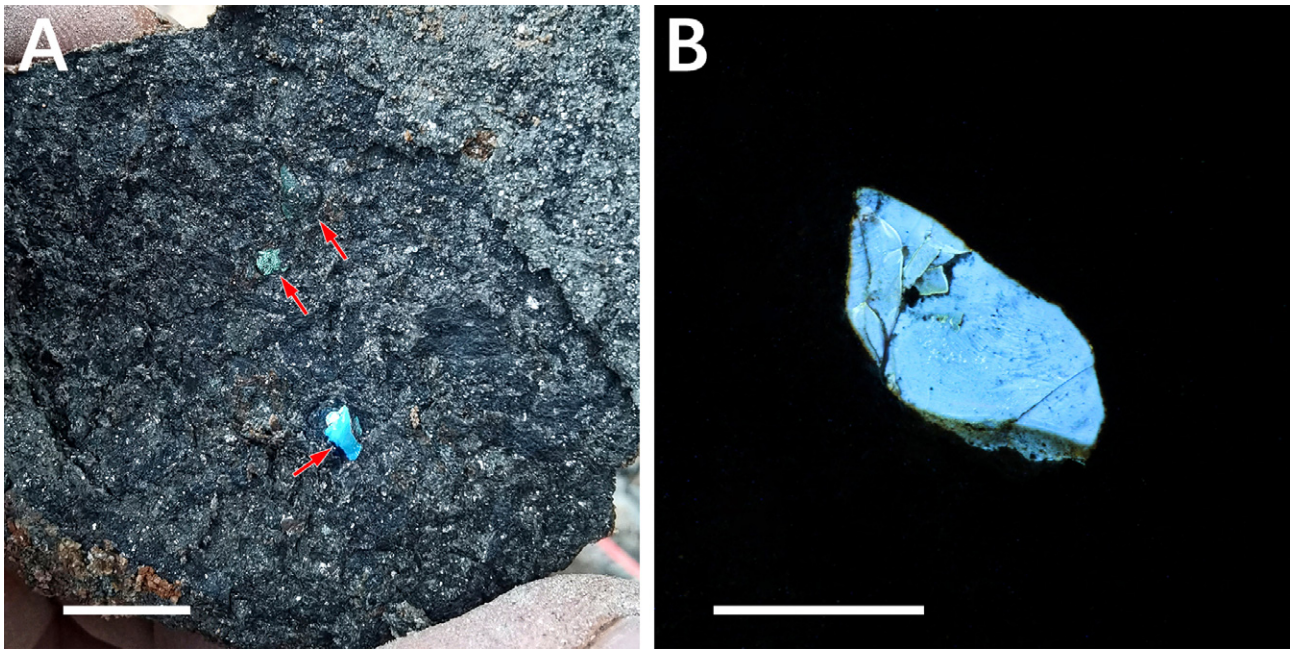

FIGURE 6. Fluorescence of Xixia amber. The red arrows indicate ambers. Scale bars = 1 cm in **A**, 0.5 cm in **B**.

The studied spectra can be categorized into three groups based on their spectral topologies: 1) Group 1: Includes amber from Xipingya, Daxigou, and Sigou (Fig. 7A–C); 2) Group 2: Includes amber from Zhaoxingou Tunnel (Fig. 7D); and 3) Group 3: Includes amber from Muzhai, Huangshi, Liying Tunnel, Caoying Tunnel, and Xingou Tunnel (Fig. 7E–I).

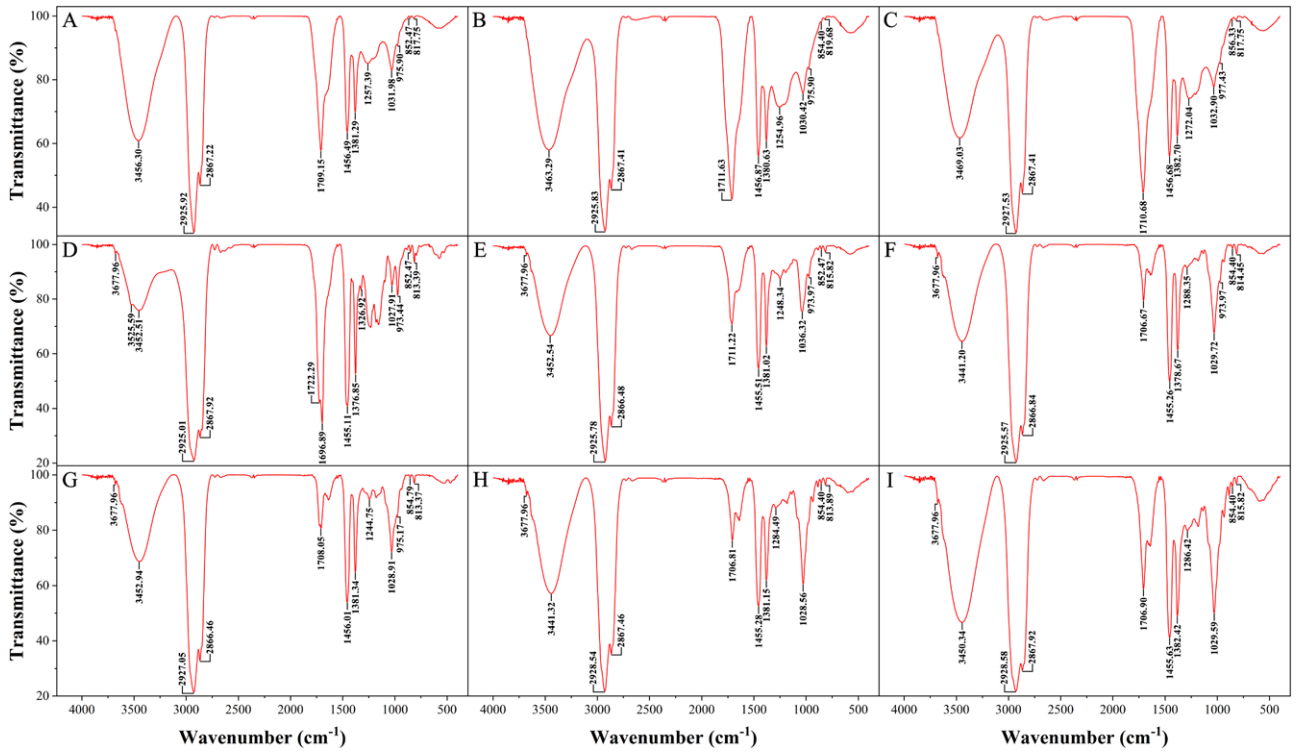

FIGURE 7. FT-IR spectra of Xixia amber. **A**, Amber from Xipingya. **B**, Amber from Daxigou. **C**, Amber from Sigou. **D**, Amber from Zhaoxingou Tunnel. **E**, Amber from Muzhai. **F**, Amber from Huangshi. **G**, Amber from Liying Tunnel. **H**, Amber from Caoying Tunnel. **I**, Amber from Xingou Tunnel.

Group 1

No transmittance peak at the wavelength 3677 cm^{-1} in contrast to group 2 and 3. The strong and broad transmittance peak at the wavelengths 3456–3469 cm^{-1} correspond to O–H stretching in alcohol and/or carboxylic acid. Transmittance peaks at the wavelengths 2925–2927 and 2867 cm^{-1} correspond to C–H stretching in CH, CH_2 and CH_3. Transmittance peak at the wavelengths 1709–1711 cm^{-1} corresponds to C=O stretching in carboxylic acids. Transmittance peak at the wavelength 1456 cm^{-1} corresponds to C–H bending in CH_2 and CH_3 of alkyl groupings. Transmittance peak at the wavelengths 1380–1382 cm^{-1} corresponds to C–H bending in CH_3 of alkyl groupings. Transmittance peak at the wavelengths 1254–1272 cm^{-1} corresponds to C–O stretching in alkyl aryl ether. Transmittance peak at the wavelengths 1030–1032 cm^{-1} corresponds to C–O stretching in alkyl aryl ether. The transmittance peak at the wavelength 975 cm^{-1} corresponds to C–H bending in CH_2 of cycloalkane. The transmittance peaks at the wavelengths 852–856 and 815–817 cm^{-1} correspond to C–H bending.

Group 2

The weak transmittance peak at the wavelength 3677 cm^{-1} correspond to low concentration of O–H stretching in alcohol or phenol. The weak transmittance peak at the wavelength 3525 cm^{-1} corresponds to correspond to O–H stretching in alcohol. The strong and broad transmittance peak at the wavelength 3452 cm^{-1} correspond to O–H stretching in alcohol and/or carboxylic acid. Transmittance peaks at the wavelengths 2925 and 2867 cm^{-1} correspond to C–H stretching in CH, CH_2 and CH_3. The transmittance peak at the wavelength 1722 cm^{-1} corresponds to C–H bending in aromatic compound, this peak is absent in group 1 and 2. Transmittance peak at the wavelength 1696 cm^{-1} corresponds to C=O stretching in conjugated aldehyde. Transmittance peak at the wavelength 1455 cm^{-1} corresponds to C–H bending in CH_2 and CH_3 of alkyl groupings. Transmittance peak at the wavelength 1376 cm^{-1} corresponds to C–H bending in CH_3 of alkyl groupings. Transmittance peak at the wavelength 1326 cm^{-1} corresponds to N–O symmetric stretching in nitro compound. Transmittance peak at the wavelength 1031 cm^{-1} corresponds to C–O stretching in

alkyl aryl ether. The transmittance peak at the wavelength 973 cm^{-1} corresponds to C–H bending in CH_2 of cycloalkane. The transmittance peaks at the wavelengths 852 and 813 cm^{-1} correspond to C–H bending.

Group 3

The weak transmittance peak at the wavelength 3677 cm^{-1} in the four spectra correspond to low concentration of O–H stretching in alcohol or phenol. The strong and broad transmittance peak at the wavelengths 3441, 3452, 3441, 3450, 3452 cm^{-1} in respectively Huangshi, Muzhai, Caoying Tunnel, Xingou Tunnel and Liying Tunnel, correspond to O–H stretching in alcohol and/or carboxylic acid. Transmittance peaks at the wavelengths 2925–2928 and 2866–2867 cm^{-1} correspond to C–H stretching in CH, CH_2 and CH_3. Transmittance peak at the wavelengths 1706–1711 cm^{-1} corresponds to C=O stretching in carboxylic acids. Transmittance peak at the wavelength 1455 cm^{-1} corresponds to C–H bending in CH_2 and CH_3 of alkyl groupings. Transmittance peak at the wavelengths 1378–1382 cm^{-1} corresponds to C–H bending in CH_3 of alkyl groupings. Transmittance peak at the wavelengths 1028–1036 cm^{-1} correspond to C–O stretching in alkyl aryl ether. The transmittance peak at the wavelengths 973–975 cm^{-1} correspond to C–H bending in CH_2 of cycloalkane. The transmittance peaks at the wavelengths 852–854 and 813–815 cm^{-1} correspond to C–H bending.

All these detected functional groups in the three groups of spectra indicate the large dominance of the aliphatic chains in the chemical constitution of the studied amber from the different outcrops. It is noteworthy that the infrared analyses have long been used in amber characterisation; however, used alone, they cannot be necessarily precise in correctly ascertaining the botanical origin of the amber.

Conclusion

Here, we present a preliminary analysis of the characteristics of amber from the Gaogou Formation in the Xixia Basin. Some researchers have suggested that the Xixia amber originated from Late Triassic strata in the northern or northwestern regions of the basin (Zhou *et al*., 2005). During deposition, resin production was abundant, and the resin exhibited high fluidity. While still unconsolidated, it was transported and mixed with sedimentary materials such as sand and mud, though without undergoing long-distance transport. The discovery of autochthonously preserved amber from Xipingya in Wuliqiao Town, as reported in this study, suggests that the amber did not originate from the basin's periphery but rather from source closely associated with the depositional layers.

Currently, there is insufficient evidence to precisely date the Late Cretaceous strata containing amber in the Xixia Basin. Additionally, no bioinclusions have been identified in the Xixia amber to date. Future research may yield new discoveries and provide deeper insights into the origin and significance of this remarkable amber deposit.

Acknowledgements

We are grateful to the two anonymous reviewers for their valuable comments on the previous version of this manuscript. This work was supported by the National Key Research and Development Program of China (2024YFF0807601) and the National Natural Science Foundation of China (41925008, 42172030 and 42288201).

References

Azar, D., Gèze, R. & Acra, F. (2010) Chapter 14: Lebanese amber. *In*: Penney, D. (Ed.), *Biodiversity of fossils in amber from the major World deposits*. Siri Scientific Press, Manchester, pp. 271–298.

Azar, D., Maksoud, S., Cai, C.Y. & Huang, D.Y. (2019) A new amber outcrop from the Lower Cretaceous of northeastern China. *Palaeoentomology*, 2 (4), 345–349. https://doi.org/10.11646/palaeoentomology.2.4.8

Cao, M.Z. & Wang, D.Y. (2011) Late Cretaceous non-marine Ostracoda from the dinosaur egg-bearing strata of Xixia basin, Henan, China. *Acta Palaeontologica Sinca*, 46 (3), 299–313. [In Chinese]

Chai, Y. & Huang, B. (2011) The behavior of thermal variation about the emperor from Xixia, Henan. *Superhard Material Engineering*, 23 (1), 56–61. [In Chinese]

Chen, J.H., Wang, D.Y., Feng, J.C., Fu, G.H. & Zhu, S.G. (2007) Late Cretaceous non-marine bivalves from the dinosaur egg-bearing strata of Xixia basin, Henan, China. *Acta Palaeontologica Sinca*, 46 (3), 299–313. [In Chinese]

Delclòs, X., Peñalver, E., Barrón, E., Peris, D., Grimaldi, D.A., Holz, M., Labandeira, C.C., Saupe, E.E., Scotese, C.R., Solórzano-Kraemer, M.M., Álvarez-Parra, S., Arillo, A., Azar, D., Cadena, E.A., Corso, J.D., Kvaček, J., MonleónGetino, A., Nel, A., Peyrot, D., Bueno-Cebollada, C.A., Gallardo, A., González-Fernández, B., Goula, M., Jaramillo, C., Kania-Kłosok, L., Valle, R.L., Lozano, R P., Meléndez, N., Menor-Salván, C., Peña-Kairath, C., Perrichot, V., Rodrigo, A., Sánchez-García, A., Santer, M., Sarto i Monteys, V., Uhl, D., Viejo, J.L. & Pérez-de la Fuente, R. (2023) Amber and the Cretaceous resinous interval. *Earth-Science Reviews*, 243, 104486. https://doi.org/10.1016/j.earscirev.2023.104486

Gao, H.L., Su, Y.T., Cai, C.Y. Azar, D., Song, X.B., Lian, X.N.

& Huang, D.Y. (2024) Discussion on the age of the Early Cretaceous amber from the Hailar Basin, NE China. *Mesozoic*, 1 (2), 192–207.
https://doi.org/10.11646/mesozoic.1.2.11

He, Q., Yang, S., Jia, S.H., Xu, L., Xing, L.D., Gao, D.S., Liu, D., Gao, Y.L. & Zheng, Y.L. (2020) Trace element and isotope geochemistry of macroelongatoolithid eggs as an indicator of palaeoenvironmental reconstruction from the Late Cretaceous Xixia Basin, China. *Cretaceous Research*, 109, 104373.
https://doi.org/10.1016/j.cretres.2020.104373

Henan Provincial Bureau of Geology and Mineral Resources. (1997) *Lithologic stratigraphy of Henan Province*. China University of Geosciences Press, Wuhan, 299 pp. [In Chinese]

Li, Y.F., Cai H.A., Liang, H.D., Zhang, J., Mei, Y.Q. & Zhang, H.G. (2006) A study on the macro mineral compositions of the dinosaur egg fossils in the Late Cretaceous collected from Xixia Basin, Henan Province. *Journal of Jilin University (Earth Science Edition)*, 36 (2), 158–163+168. [In Chinese]
https://doi.org/10.13278/j.cnki.jjuese.2006.02.002

Li, Y., Feng, Y.L., Du, J.F., Wang, Y.M., Shi, G.H. & Liang, Y.Z. (2024) Spectral and chemical characterization of amber from Xixia, Henan Province, China via FTIR, three-dimensional fluorescence spectra and Py (HMDS)-GC-MS. *Heliyon*, 10 (16), e35066.
https://doi.org/10.1016/j.heliyon.2024.e35066

Li, Y.L., Zheng, D.R., Sha, J.G., Zhang, H.C., Denyszyn, S. & Chang, S.C. (2023) Lower Cretaceous Hailar amber: The oldest-known amber from China. *Cretaceous Research*, 145, 105472.
https://doi.org/10.1016/j.cretres.2022.105472

Ni, Z.J., Song, X.B., Azar, D., Wang, Z.X., Cai, C.Y., Xuan, Q., Maksoud, S., Lian, X.N. & Huang, D.Y. (2023) Discovery of Late Cretaceous amber from Guangzhou, South China. *Palaeoentomology*, 6 (4), 329–332.
https://doi.org/10.11646/palaeoentomology.6.4.3

Shi, G.L., Dutta, S., Paul, S., Wang, B. & Jacques, F.M.B. (2014) Terpenoid compositions and botanical origins of Late Cretaceous and Miocene amber from China. *PLoS One*, 9 (10), e111303.
https://doi.org/10.1371/journal.pone.0111303

Song, X.B., Sui, X., Xuan, Q., Azar D., Cai, C.Y., Wang Z.X. & Huang D.Y. (2024) A new amber outcrop from the Late Cretaceous of Xingning Basin, South China. *Palaeoentomology*, 7 (6), 770–777.
https://doi.org/10.11646/palaeoentomology.7.6.12

Wang, B., Rust, J., Engel, M.S., Szwedo, J., Dutta, S., Nel, A., Fan, Y., Meng, F.W., Shi, G.L., Jarzembowski, E.A., Wappler, T., Stebner, F., Fang, Y., Mao, L.M., Zheng, D.R. & Zhang, H.C. (2014) A diverse paleobiota in Early Eocene Fushun amber from China. *Current Biology*, 24 (14), 1606–1610.
https://doi.org/10.1016/j.cub.2014.05.048

Wang, B., Shi, G.L., Xu, C.P. Spicer, R.A., Perrichot, V., Schmidt, A.R., Feldberg, K., Heinrichs, J., Chény, C., Pang, H., Liu, X.Y., Gao, T.P., Wang, Z.X., Ślipiński, A., Solórzano-Kraemer, M.M., Heads, S.W., Thomas, M.J., Sadowski, E.M., Szwedo, J., Azar, D., Nel, A., Liu, Y., Chen, J., Zhang, Q., Zhang, Q.Q., Luo, C.H., Yu, T.T., Zheng, D.R., Zhang, H.C. & Engel, M.S. (2021) The mid-Miocene Zhangpu biota reveals an outstandingly rich rainforest biome in East Asia. *Science Advances*, 7, eabg0625.
https://doi.org/10.1126/sciadv.abg0625

Wang, D.Y., Feng, J.C., Zhu, S.G., Wu, M., Fu, G.H., He, P., Qiao, G.C., Pang, J.F., Li, G.W., Li, B.X., Li, J., Wang, B.X., Zhang, G.J., Qin, Z. & Guo, G.L. (2008) *The dinosaur eggs and dinosaur fossils in Henan Province, China*. Geology Press, Beijing, 320 pp. [In Chinese]

Wang, H.S. (1989) A mineralogical study of Amber from Xixia region, Hennan province. *Acta Mineralogica Sinica*, 9 (4), 338–344+387. [In Chinese]
https://doi.org/10.16461/j.cnki.1000-4734.1989.04.008

Wang, X.L., Wang, Q., Jiang, S.X., Cheng, X., Zhang, J.L., Zhao, Z.K. & Jiang, Y.G. (2012) Dinosaur egg faunas of the Upper Cretaceous terrestrial red beds of China and their stratigraphical significance. *Journal of Stratigraphy*, 36 (2), 400–416.
https://doi.org/10.19839/j.cnki.dcxzz.2012.02.017

Wang, X.W., Yao, X.Y. & Xu, X.Y. (2015) Trace element determination of Late Cretaceous dinosaur eggshell fossils from Xixia Basin, Henan Province by ICP-OES and Its Implications for Extinction of Dinosaurs. *Rock and Mineral Analysis*, 34 (5), 520–527. [In Chinese]
https://doi.org/10.15898/j.cnki.11-2131/td.2015.05.004

Yang, W.R. (1987) "Opening" and "closing" history in east Qinling era. *Earth Science*, 12 (5), 487–493. [In Chinese]

Zhang, Y.G. & Pei, J. (2004) Trace element combinations in Upper Cretaceous dinosaur egg fossils from Xixia Basin and discussion on paleoclimate. *Acta Palaeontologica Sinica*, 43 (2), 297–302. [In Chinese]

Zhong, H.B. (2003) Amber resources of China. *Journal of Gems and Gemmology*, 5 (2), 33. [In Chinese]
https://doi.org/10.15964/j.cnki.027jgg.2003.02.012

Zhou, S.Q. & Zhao, S.L. (2005) Initial study on the Xixia-Neixiang amber deposit of Henan. *Mineral Resources and Geology*, 19, 57–59. [In Chinese]

Zhou, S.Q., Feng Z.J. & Hui Y.X. (2001) A study of dinosaur and fossil eggs from the Xixia Basin, Henan. *Jiangxi Geology*, 15 (2), 96–101. [In Chinese]

Zhou, S.Q., Han, S.J. & Zhang, Y.C. (1983) The Late Cretaceous strata from Xixia Basin, Henan Province. *Journal of Stratigraphy*, 7 (1), 64–70. [In Chinese]

Zhu, G.Y. (1997) Stratigraphy and sedimentary facies of red beds in Xixia Basin of Henan Province. *Journal of the University of Petroleum, China*, 21 (6), 110–113+123. [In Chinese]